PERGAMON

Chemical Engineering Science 58 (2003) 4307–4316

Chemical Engineering Science

www.elsevier.com/locate/ces

Macroscopic modelling and identification of an anaerobic waste treatment process

J. E. Haag[a], A. Vande Wouwer[a,*], I. Queinnec[b]

[a] *Laboratoire d'Automatique, Faculté Polytechnique de Mons, 31 Boulevard Dolez, B-7000 Mons, Belgium*
[b] *Laboratoire d'Analyse et d'Architecture des Systèmes-CNRS, 7 Avenue du Colonel Roche, F-31077 Toulouse Cedex 4, France*

Received 18 June 2002; received in revised form 9 December 2002; accepted 27 May 2003

Abstract

Anaerobic fermentation is an important process used for recycling solid organic waste, which leads to a significant reduction of the waste volume with the production of biogas as a positive side effect. For state observation and control purposes, a mathematical representation of the process is required. However, anaerobic fermentation is far too complex to be described in full metabolic details, due to the variety of responsible microorganisms and the unknown and time-varying waste composition. The level of complexity of the description is limited by the amount and quality of available experimental data, which can be used for model identification. In practice, the derivation of a dynamic process model involves the following steps: (i) the selection of suitable macroscopic reaction schemes and kinetic structures, (ii) the estimation of the unknown model parameters from experimental data by minimizing a maximum-likelihood criterion, (iii) the estimation of the unknown measurement variances, (iv) the estimation of the covariance matrix of the parameter estimates and (v) the validation of the obtained model.

In this study, attention is focused on these several steps, and a dynamic model of a complex anaerobic process is inferred from infrequent measurements of global variables. The experimental data are obtained from six experiments carried out in a small-scale continuous bioreactor under different feed and (controlled) acidity conditions.

Keywords: Methanisation; Fermentation; Mathematical modelling; Parameter estimation; Environment

1. Introduction

In France, the total solid waste production is estimated at about 600×10^6 t/yr, potentially leading to significant problems of disposal space in the near future. Sorting waste with the aim of recycling reduces dump volume significantly, but is however limited to specific waste types, especially in industry. The solid organic waste fraction, distinguished by its producers into industrial, agricultural and urban, additionally incorporates sources of regenerative energy. In practice, there are two ways for recycling organic waste: by aerobic (composting) and by anaerobic fermentation (biomethanisation). The latter process leads to the production of biogas, which is directly exploitable by combustion, as a heating source or for the generation of electrical energy. The biogas yield of this biogradation depends on the waste type and varies between 100 and 200 m^3/t. Therefore it represents not only a method for reducing the amount of waste, but also an alternative for saving fossile energy sources. In addition, the controlled production and exploitation of the biogas prevents methane from entering and damaging the ozone layer in the atmosphere. More than 60 biogas production sites are currently running all over Europe.

The steadily increasing number of anaerobic waste treatment plants necessitates high technological standards in terms of process supervision and control. It is therefore of high interest to find an appropriate description of the complex bioprocess, which could be used for the estimation of important unmeasured process states. To this end, a simple model is derived in this paper, which is sufficiently general to describe different operating conditions, but is characterised by a relatively low number of model parameters. This latter feature is particularly desirable, as it allows the model to be easily adjusted to other production conditions, e.g. other types of waste.

* Corresponding author. Fax: +32-65-37-4136.
E-mail addresses: jens.haag@fpms.ac.be (J. E. Haag), alain.vandewouwer@fpms.ac.be (A. Vande Wouwer).

0009-2509/$ - see front matter © 2003 Elsevier Ltd. All rights reserved.
doi:10.1016/S0009-2509(03)00272-0

Numerous studies of specific anaerobic fermentation processes are presented in the literature, in which particular waste types such as olive mill waste (Borja, Martín, Banks, Alonso, & Chica, 1995; Fiestas Ros de Ursinos & Borja-Padilla, 1996) or animal waste (Hansen, Angelidaki, & Ahring, 1998; Simeonov, Momchev, & Grancharov, 1996). are considered, and a good qualitative knowledge, e.g. the inhibition effect of ammonia, and the influence of acidity and temperature (mesophilic and thermophilic range) has resulted. Only few approaches exist, however, for modelling the anaerobic fermentation process with respect to state observation and control. Simeonov et al. (1996) developed a dynamic three-stage model (hydrolysis, acidogenisis and methanogenisis), which is identified from methane data only and which is said to be useful for control purposes. Kiely, Tayfur, Dolan, and Tanji (1997) derived a largely parametrized model for the anaerobic digestion of municipal waste based on the modelling approach of Hill and Barth (1977), which however shows identifiability problems, when applied to a different process. A more theoretical approach is presented by Denac, Miguel, and Dunn (1988), who derive the stoichiometry of a five-reaction biodegradation chain for the treatment of molasses wastewater. It is however hardly extendable to a more complex waste composition.

Thus, no general modelling approach exists for the complex anaerobic fermentation process due to the large number of unknowns. Hence, the best strategy seems to derive an—as simple as possible—model structure incorporating the available a priori knowledge and taking specific modelling objectives (process optimisation, state estimation, control) into account. For instance, Bernard, Hadj-Sadok, and Dochain (2000) recently developed a software sensor based on a simple mass-balance model underlining the importance of advanced monitoring techniques in this field of bioprocess engineering.

This philosophy is followed in the present study, and particularly an attempt is made to answer the following question: "is it possible to develop a dynamic model of the anaerobic fermentation process from infrequent measurements of global variables?" To this end, pilot-scale experiments are carried out to cover different operating conditions (various temperatures, pH, and aqueous dilutions), and some standard analyses are made to obtain measurement data, e.g. chemical oxygen demand, material in suspension, total dry extract etc. These standard data are used to set up a simple model of the bioprocess and to estimate the unknown model parameters as well as the unknown measurement variances. By means of Fisher's information matrix, a lower bound of the covariance matrix of the estimated model parameters is calculated in order to evaluate the quality of the obtained model.

The paper is organized as follows: The bioprocess is introduced in Section 2, and the experimental conditions are detailed in Section 3. In Section 4, the mathematical model structure is derived and formulated defining the system inputs and outputs as well as the structural parameters. The identification procedure is presented in Section 5, and the results are validated and discussed. Section 6 focuses on a statistical analysis in terms of confidence in the obtained model and correlation between parameters. Concluding remarks as well as perspectives for the practical application are given in Section 7.

2. Process description

Anaerobic fermentation is a complex process, in which many reactions take place. Due to the time-varying waste composition, experiments are seldom reproducible, and a detailed physical description of the process is usually intractable. Rather, it is in most cases more appropriate to investigate the process in a macroscopic way. To this end, the waste composition is classified according to

- organic vs. inorganic,
- particulate vs. dissolved,
- long- vs. short-chained molecules.

In the methanisation process, the organic waste degrades biologically to produce volatile fatty acids and biogas, a mixture of methane and carbon dioxide. Different types of bacteria, which sequentially break down the organic parts of the waste in several steps, are responsible for the biodegradation:

- In a first step, the particulate organic components characterized by long-chained molecules of carbohydrates, lipids and proteins, are solubilized by *hydrolysis*. This initial degradation step is performed by bacteria called *hydrolytic* biomass. The existence of this distinct type of bacteria is however doubted in the literature (Borzacconi, Lòpez, & Anido, 1997; Angelidaki, Ellegaard, & Ahring, 1999) where it is considered that hydrolysis is catalysed by enzymes commonly excreted by various bacteria.
- The second step in the biodegradation process is believed to be bio-catalyzed by the *acidogenic* bacteria. The medium-chained product molecules of hydrolysis are converted into volatile fatty acids consisting of short carbon chains (C_2–C_5).
- The (mainly acetic) volatile fatty acids represent substrates for the third step performed by the *methanogenic* bacteria, which convert them into the biogas components methane and carbon dioxide.

3. Experiments

A series of experiments with different waste types were carried in eight small-scaled reactors running in parallel under different experimental conditions. The bioreactors of volume $V = 11$ were run in (quasi-) continuous mode with

Table 1
Experimental conditions of the series of six experiments

Exp. no.	1	2	3	4	5	6
p_H (dimensionless)	5.5	6.0	6.5	7.0	6.0	6.5
T (°C)	35	35	35	35	35	35
t_{end} (d)	44	44	44	44	38	65
Samples (dimensionless)	13	13	13	13	12	18

Table 2
Some measured feed concentrations of organic fraction of urban household refuse

Exp. no.	1	2	3	4	5	6a	6b
Chemical oxygen demand (g/l)	20.0	20.0	20.0	20.0	20.0	50.0	112.0
Total organic carbon (g/l)	1.7	1.7	1.7	1.7	1.7	4.3	9.5
Material in suspension (g/l)	21.3	21.3	21.3	21.3	21.3	53.3	119.3
Total dry extract (g/l)	23.1	23.1	23.1	23.1	23.1	57.8	129.5

a daily replacement rate of 10 percent of reactor content by new waste suspension, i.e. $D = 0.1$ l/d, applied discontinuously once per day. In this contribution, only the results obtained for the organic fraction of household refuse belonging to the urban waste are considered. Six experiments of 38–65 days duration were evaluated by taking samples twice a week. The reactors were inoculated with sludge from another anaerobic digestion process treating waste from wine production. All experiments were carried out at non-limiting concentrations of nitrogen (NTK > 0.5 g/l) and phosphorus ($P_t > 0.3$ g/l) sources. The samples were analysed according to a protocol yielding important biological variables, e.g. chemical oxygen demand (COD), total organic carbon (TOC) and some volumic mass concentrations. The experimental conditions are summarized in Table 1.

For mathematical modelling purposes, the experiments were carried out with different operating conditions, i.e. the pH was varied from one experiment to another, but was regulated during each run by addition of a bicorbonate solution. The temperature was maintained at 35°C by a warm water jacket. In addition, the experiments cover three feed conditions differing in their dilution Table 2.

4. Modelling

The experimental data cannot give a detailed insight into the biological process, since the measurements lump together several components and give therefore only a global view. Especially the segregation of biomass is delicate because there is no accessible quantitative measure for the different compartments. For this reason, the modelling approach is essentially macroscopic.

The derivation of the model structure is introduced in the sequel.

4.1. Measurements

Samples of the feed as well as of the reactor content were analysed resulting in seven biochemically important numbers.

In a first step of the analysis, one fraction is centrifugated to eliminate the solid content before further analysis; the other fraction is analysed with its components in suspension.

Both fractions are dryed at 105°C to eliminate the solvent and then burned at 500°C. The COD for oxidation of the dry material is determined, resulting in a biological key measure of the organic content in the sample.

Organic material usually fits the general formula $C_\alpha H_\beta O_\gamma N_\delta$. During its combustion, the carbon, hydrogen and nitrogen atoms are converted into their highest stage of oxidation through the following chemical reaction:

$$C_\alpha H_\beta O_\gamma N_\delta + \left(\alpha + \frac{\beta}{4} - \frac{\gamma}{2} + \delta\right) O_2 \rightarrow \alpha CO_2 + \frac{\beta}{2} H_2O + \delta NO_2. \quad (1)$$

In the ideal case of complete oxidation, the COD is calculated in terms of the corresponding mass (c) by

$$\Omega^{-1} = \frac{c}{\mathrm{COD}} = \frac{\alpha M_C + \beta M_H + \gamma M_O + \delta M_N}{(2\alpha + \frac{\beta}{2} - \gamma + 2\delta) M_O} \ \text{in} \ \frac{\mathrm{g}}{\mathrm{gCOD}}. \quad (2)$$

Ω has typical values between 1 to 3 gCOD/g.

The TOC content is another representative measure of the organic material. It is determined for the centrifugated fraction and represents the mass of all carbon atoms present in the sample. The conversion between the TOC number

and mass is calculated analogously to the COD by

$$\Gamma^{-1} = \frac{c}{\mathrm{TOC}} = \frac{\alpha M_C + \beta M_H + \gamma M_O + \delta M_N}{\alpha M_C}. \quad (3)$$

Typical values for Γ are between 0.4 and 0.8 gTOC/g.

The remaining measurements have the following physical meanings:

- The *material in suspension (MiS)* is the mass difference of the centrifugated fraction before and after centrifugation.
- The *total dry extract (TDE)* is the mass of the dried non-centrifugated fraction.
- The *organic dry extract (ODE)* represent the mass difference between the residuals of the non-centrifugated fraction after drying and burning, respectively.
- The overall *volatile fatty acid (VFA)* concentration—including acetic (C_2) to valeric acid (C_5)—is determined by gas chromatography.

Consequently, the measurement vector $\mathbf{y}$ consists of seven elements:

$$\mathbf{y}^{\mathrm{T}} = [\mathrm{COD}_s\ \mathrm{COD}_t\ \mathrm{MiS}\ \mathrm{TDE}\ \mathrm{ODE}\ \mathrm{TOC}\ \mathrm{VFA}]. \quad (4)$$

Biogas, and more specifically the produced amounts of methane and carbon dioxide, were not measured due to the lack of reliable quantitative methods. The main objective of this study is to focus attention on the reduction of the amount of solid organic waste through the anaerobic fermentation process. Furthermore, this study is motivated by the attempt of a simple modelling approach from standard measurements, even without the data of the produced biogas.

4.2. States

The proposed model contains states, which are assumed to characterize the dynamic behaviour of the real system appropriately well. Due to the lack of measurements of single concentrations, the dynamics are represented by the concentrations of the following components classified according to their physico-chemical properties in the state vector:

$$\mathbf{x} = \begin{bmatrix} X_a \\ X_m \\ X_S \\ X_I \\ S_S \\ S_I \\ S_{\mathrm{VFA}} \end{bmatrix} \begin{matrix} \ldots \text{acidogenic biomass,} \\ \ldots \text{methanogenic biomass,} \\ \ldots \text{solid hydrolysable substrate,} \\ \ldots \text{inert solid material,} \\ \ldots \text{easily biodegradable substrate,} \\ \ldots \text{inert dissolved material,} \\ \ldots \text{volatile fatty acids} \end{matrix} \quad (5)$$

containing $n_x = 7$ elements, where X denotes the concentration of particles in suspension and S the concentration of a dissolved component (each in g/l).

Even though they are not affected by biodegradation, the inert solid X_I and dissolved components S_I are considered in this representation, as they are present in the measurement signals.

The gaseous products methane and carbon dioxide are not considered, since their measurements are not available. It is assumed that their production is linearly related to the methanogenic step.

Previous studies (Gérin, 2000) have shown that the consideration of three types of biomass with the global measurement data described in Section 4.1 leads to strong practical identifiability problems. These problems can be (at least partly) alleviated by lumping together the biomass responsible for hydrolysis and acidogenesis (Borzacconi et al., 1997; Angelidaki et al., 1999).

Note that there is no direct way to calculate the state directly from these global measurements.

4.3. Reaction scheme

According to the sequential biodegradation, there are three main reactions in series, in which two types of biomass are involved. It is assumed that the acidogenic and the methanogenic steps are growth-associated:

$$X_S \overset{\varphi_h X_a}{\rightarrow} S_S, \quad (6)$$

$$\left(\frac{1}{Y_a}\right) S_S \overset{\varphi_a X_a}{\rightarrow} X_a + \left(\frac{1}{Y_a} - 1\right) S_{\mathrm{VFA}}, \quad (7)$$

$$\left(\frac{1}{Y_m}\right) S_{\mathrm{VFA}} \overset{\varphi_m X_m}{\rightarrow} X_m + \frac{1}{Y_{\mathrm{CH_4}}}\,\mathrm{CH_4} + \frac{1}{Y_{\mathrm{CO_2}}}\,\mathrm{CO_2}. \quad (8)$$

The specific reaction rates are formulated using Monod's classical law (Monod, 1942):

$$\varphi_h = \varphi_{h,\max}\,(p_H, T, \ldots)\frac{X_S}{X_S + K_{X_S}}, \quad (9)$$

$$\varphi_a = \varphi_{a,\max}\,(p_H, T, \ldots)\frac{S_S}{S_S + K_{S_S}}, \quad (10)$$

$$\varphi_m = \varphi_{m,\max}\,(p_H, T, \ldots)\frac{S_{\mathrm{VFA}}}{S_{\mathrm{VFA}} + K_{S_{\mathrm{VFA}}}} \quad (11)$$

characterized by the rate-limitation of at least one substrate.

In analogy to enzymatic reactions, the following expression for the p_H dependence of the methanogenesis is derived (Borzacconi et al., 1997; Lay, Li, Noike, Endo, & Ishimoto, 1997; Bailey & Ollis, 1996):

$$\varphi_{m,\max} = \frac{(ke_0)_m}{1 + 10^{-p_H + p_{K_1}} + 10^{p_H - p_{K_2}}}, \quad (12)$$

where e_0 denotes the catalyzing key enzyme activity and $p_K = -\lg K$. The optimum p_H, i.e. the condition for the

maximum growth rate with respect to the p_H is given by

$$p_{H,\mathrm{opt}} = \frac{1}{2}(p_{K_1} + p_{K_2}). \tag{13}$$

In addition, biomass dies or becomes inactive with an assumed-constant specific death rate k_d. Since the cells mainly consist of solid organic material, dead biomass is fully recycled as nutrient in the hydrolysis:

$$X_a \overset{k_{d,a}X_a}{\longrightarrow} X_S, \tag{14}$$

$$X_m \overset{k_{d,m}X_m}{\longrightarrow} X_S. \tag{15}$$

4.4. Model equations

The model equations can be written in the general form

$$\dot{\mathbf{x}}(t) = \mathbf{K}\mathbf{r}(\mathbf{x}(t)) + D[\mathbf{x}_{\mathrm{in}} - \mathbf{x}(t)], \quad \mathbf{x}(t=0) = \mathbf{x}_0, \tag{16}$$

$$\mathbf{y}(t) = \mathbf{C}\mathbf{x}(t), \tag{17}$$

where $\mathbf{K}$ is the stoichiometric matrix

$$\mathbf{K} = \begin{bmatrix} 0 & 1 & 0 & -1 & 0 \\ 0 & 0 & 1 & 0 & -1 \\ -1 & 0 & 0 & 1 & 1 \\ 0 & 0 & 0 & 0 & 0 \\ 1 & -\frac{1}{Y_a} & 0 & 0 & 0 \\ 0 & 0 & 0 & 0 & 0 \\ 0 & \frac{1}{Y_a} - 1 & -\frac{1}{Y_m} & 0 & 0 \end{bmatrix} \tag{18}$$

and $\mathbf{r}$ is the reaction rate vector

$$\mathbf{r} = \begin{bmatrix} \varphi_h X_a \\ \varphi_a X_a \\ \varphi_m X_m \\ k_{d,a} X_a \\ k_{d,m} X_m \end{bmatrix}. \tag{19}$$

$\mathbf{x}_{\mathrm{in}}$ is the concentration vector of the incoming waste, $\mathbf{x}_0$ is the vector of initial concentrations in the reactor, and D is the dilution rate. The constant measurement matrix $\mathbf{C}$ is written as

$$\mathbf{C} = \begin{bmatrix} 0 & 0 & 0 & 0 & \Omega_{S_S} & 0 & \Omega_{S_{\mathrm{VFA}}} \\ \Omega_{X_X} & \Omega_{X_X} & \Omega_{X_S} & 0 & 0 & 0 & 0 \\ 1 & 1 & 1 & 1 & 0 & 0 & 0 \\ 1 & 1 & 1 & 1 & 1 & 1 & 1 \\ 1 & 1 & 1 & 0 & 1 & 0 & 1 \\ 0 & 0 & 0 & 0 & \Gamma_{S_S} & 0 & \Gamma_{S_{\mathrm{VFA}}} \\ 0 & 0 & 0 & 0 & 0 & 0 & 1 \end{bmatrix}. \tag{20}$$

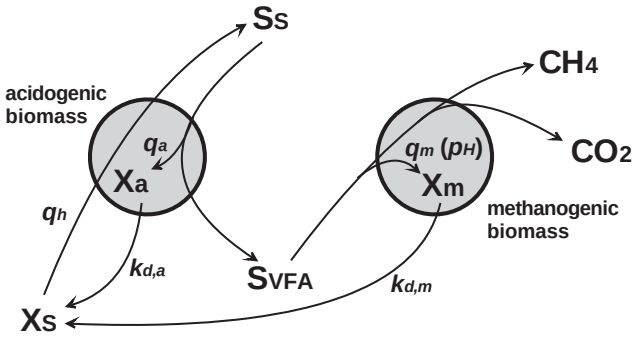

Fig. 1. Considered reaction scheme.

The global macroscopic reaction scheme is depicted in Fig. 1.

4.5. Model parameters

The parameter vector contains 44 elements:

$$\begin{aligned} \mathbf{p}^{\mathrm{T}} = [&\mathbf{x}_{\mathrm{in}}^{*\mathrm{T}}\ \mathbf{x}_{0,1-4}^{\mathrm{T}}\ \mathbf{x}_{0,5}^{\mathrm{T}}\ \mathbf{x}_{0,6}^{\mathrm{T}}\ \cdots \\ &\cdots\ Y_a\ Y_m\ \varphi_{h,\max}\ \varphi_{a,\max}\ \varphi_{m,\max}\ k_{d,a}\ k_{d,m}\ \cdots \\ &\cdots\ K_{X_S}\ K_{S_S}\ K_{S_{\mathrm{VFA}}}\ p_{K,1}\ p_{K,2}\ \cdots \\ &\cdots\ \Omega_{X_X}\ \Omega_{X_S}\ \Omega_{S_S}\ \Omega_{S_{\mathrm{VFA}}}\ \Gamma_{S_S}\ \Gamma_{S_{\mathrm{VFA}}}] \end{aligned} \tag{21}$$

and is generally classified into three parts:

- the feed ($\mathbf{x}_{\mathrm{in}}^{*\mathrm{T}} = [X_{S,f}\ X_{I,f}\ S_{S,f}\ S_{I,f}\ S_{\mathrm{VFA},f}]$) and initial states ($\mathbf{x}_0$) as experimental parameters—26 unknowns,
- the model parameters including stoichiometric (Y), kinetic ($\varphi_{\max}, (ke_0)_m, k_d$) and saturation constants (K, p_K) as structural model parameters—12 unknowns,
- the conversion factors for COD (Ω) and for TOC (Γ) as measurement parameters—6 unknowns.

The yield coefficients of the biogas components CH_4 and CO_2 cannot be determined in this model identification due to the absence of measurement of the gaseous products.

Note that the initial conditions of the experiments 1–4 ($\mathbf{x}_{0,1-4}$) are the same, whereas the initial concentrations for experiments 5 and 6 are different ($\mathbf{x}_{0,1-4} \neq \mathbf{x}_{0,5} \neq \mathbf{x}_{0,6}$). Furthermore, the aqueous dilution factor of the feed waste is known for each experiment. It is therefore sufficient to estimate the elements of only one reference feed concentration vector $\mathbf{x}_{\mathrm{in}}$.

5. Identification

The unknown model parameters are now estimated from the experimental data.

5.1. Cost function

In order to find the best fit of a model to given experimental data, an appropriate criterion for the optimal solution of the model parameter vector must be selected.

A general criterion for noisy data is the maximum-likelihood criterion

$$\hat{\mathbf{p}} = \arg\max_{\mathbf{p}} \{P[\mathbf{y}_i|\mathbf{p}]\}. \tag{22}$$

This criterion maximizes the likelihood of the measurement data set $\mathbf{y}_i$ with respect to the parameter vector $\mathbf{p}$. It is derived from the Bayesian estimator assuming no a priori knowledge on the parameters, i.e. a uniform probability distribution for the parameter vector.

The well-known weighted-least-squares criterion of the Gauss–Markov estimator is derived from the maximum-likelihood cost function under the following assumptions (Walter & Pronzato, 1997):

- the inputs and states are noise-free;
- the measurement error is uncorrelated, white, i.e. uncorrelated from one sampling instant to another, and normally distributed, i.e. with a zero mean value and a Gaussian distribution;
- the measurement error is known at each sampling instant and independent of the states.

The Gauss–Markov criterion is then written:

$$\hat{\mathbf{p}} = \arg\min_{\mathbf{p}} \{j_{\mathrm{wls}}\} \tag{23}$$

with the cost function defined as

$$j_{\mathrm{wls}} = \sum_{i=1}^{n_t} [\mathbf{y}_i - \mathbf{y}_m(\mathbf{x}(t_i, \mathbf{p}), t_i, \mathbf{p})]^{\mathrm{T}} \times \boldsymbol{\Sigma}_i^{-1} [\mathbf{y}_i - \mathbf{y}_m(\mathbf{x}(t_i, \mathbf{p}), t_i, \mathbf{p})]. \tag{24}$$

This criterion requires the diagonal measurements (co-) variance matrix $\boldsymbol{\Sigma}_i$, which is however often not known a priori. In this case, the elements $\sigma_j(t_i)$ also have to be included in the vector of unknown parameters, dramatically increasing the problem dimensionality.

To alleviate this problem, consider the following parametrized form of the diagonal measurement covariance matrix representing a relative measurement error:

$$\boldsymbol{\Sigma}_i = \mathrm{diag}\{\boldsymbol{\Sigma}_{\mathrm{rel}} \mathbf{y}_m(t_i)\}, \tag{25}$$

which is now a linear function of the ideal output $\mathbf{y}_m = \mathbf{C}\mathbf{x}$. The proportionality matrix $\boldsymbol{\Sigma}_{\mathrm{rel}}$ is time-invariant and contains the unknown elements $\sigma^2_{\mathrm{rel},j}$ in its main diagonal. An analytical expression can be derived from the optimality condition for $\boldsymbol{\Sigma}_{\mathrm{rel}}$, and included in the cost function such that the parameter dimension is reduced to its original size and the cost function implicitly includes the unknown variances (Goodwin & Payne, 1977). This leads to the following form of the maximum-likelihood optimality criterion:

$$j_{ml}(\mathbf{p}) = \sum_{j=1}^{n_y} \left\{ n_{t,j} \ln\{\hat{\sigma}_{\mathrm{rel},j}(\mathbf{p})\} + 2 \sum_{i=1}^{n_{t,j}} \ln\{y_{m,j}(t_{ji}, \mathbf{p})\} \right\} \tag{26}$$

with the estimated relative variances

$$\hat{\sigma}_{\mathrm{rel},j}(\mathbf{p}) = \frac{1}{n_{t,j}} \sum_{i=1}^{n_{t,j}} \left(\frac{y_{ji} - y_{m,j}(t_{ji}, \mathbf{p})}{y_{m,j}(t_{ji}, \mathbf{p})} \right)^2. \tag{27}$$

In contrast to the (weighted-)least-squares cost function of the Gauss–Markov estimator, no dedicated algorithms, like e.g. the Levenberg–Marquardt method, can be used to find the optimum of this non-linear problem, but a general minimum-seeking algorithm has to be applied. A short introduction is given in the next section.

5.2. Optimization method

There exists a large variety of structurally different methods to solve optimisation problems. None of them can generally be said to be the best a priori since, depending on the problem structure, some methods might be more advantageous than others.

In this study, the optimisation problem is non-linear and non-convex. Such problems generally do not have a guaranteed single optimum. It is therefore desired to obtain the global among all the other local optima, which refers to the class of global optimisation problems, currently subject of major interest in mathematical science. A well-known and widely-used flexible method to find a global optimal solution is the *Simulated Annealing* strategy (Kirkpatrick, Gelatt, & Vecchi, 1983). The reduction of the search radius along the optimisation progress results in a final solution with a high probability to be the global optimum. Global search methods, however, suffer from a relatively large tuning parametrisation (and high computational load) and are usually less performant in locating a minimum in terms of rate of convergence, since the parameter domain is scanned more extensively and less efficiently towards decreasing cost function values.

The gradient-based methods (Nocedal & Wright, 1999), like the *(modified) Newton* algorithm, are classically restricted to local minimum seeking, since they follow the slope to arrive at the optimum point. They make use of the gradient at the intermediate solution after each iteration. Therefore, only the local vicinity is evaluated, often applying the assumption of convexity of the problem, which is not the case here. The gradient is in most cases computed numerically, either by finite differences or by numerical integration of the sensitivities, since the analytical solution does not exist.

On the other hand, the direct-search methods (Powell, 1998) are not based on the gradient, but evaluate a specific

number of parameter sets in the parameter space, which are widely and arbitrarily distributed initially. The optimisation strategy consists in reducing the size of the spanned hyperplane by dropping the parameter vector with the highest cost in favour of a new one, determined by projection. A famous example of this class of methods is the Nelder–Mead simplex method (Nelder & Mead, 1965), which is the basis of several variants proposed in the literature. Powell proposed with CObyLA (Powell, 1998) and UObyQA (Powell, 2000) two gradient-free direct search methods of first and second order, respectively.

Powell's "Unconstrained Optimization by Quadratic Approximation" algorithm (UObyQA) suits well to the present optimisation problem, since the large initial hyperplane covers nearly the complete parameter range of interest and the found optimum after reduction is therefore probable, although not guaranteed to be global. A multi-start strategy, featuring several optimisation runs from different initial parameter estimates, allows the global character of the obtained extrema to be further investigated.

The solution obtained by UObyQA is finally cross-checked with Ingber's global optimisation method "Adaptive Simulated Annealing" (ASA) (Ingber, 1996).

5.3. Parameter constraints

The parameter range of interest is set by two constraints:

- The parameters in the considered model all have a physical interpretation and are therefore constrained by zero as a lower bound. Negative values are meaningless and can have an undesirable effects on the model outputs (negative concentrations, instabilities, ...). For the same physical reasons, there is generally an upper bound, which is often set intuitively.
- Another way for setting an upper bound is the vanishing sensitivity, i.e. from a certain range of magnitude on, the impact of the parameters on the system output becomes negligibly small.

To impose bound constraints, either the parameter transformation

$$p = p_{\text{lim}} \pm \mathrm{e}^{p^*} \tag{28}$$

for a single bound p_{lim} or

$$p = 0.5\,(p_{\text{high}} + p_{\text{low}} + (p_{\text{high}} - p_{\text{low}})\tanh p^*) \tag{29}$$

for an interval $[p_{\text{low}}\ p_{\text{high}}]$ bound constraint can be used. This leads to an even more nonlinear optimization problem but prevents the algorithm from exceeding the admitted range for the original parameter p while optimizing the transformed parameter p^*. This is anyway harmless, since $\mathbf{p}^*(\mathbf{p})$ is injective. The main advantage of these transformations is that they allow an unconstrained optimisation method to be used. These latter algorithms are often simpler and more efficient than constrained methods.

Table 3
Parameter set resulting from identification: feed and initial states

$\mathbf{x}_{\text{in}}^{\text{T}} = [10.21\ 9.72\ 1.64\ 0.14\ 0.02]$	g/l
$\mathbf{x}_{01}^{\text{T}} = [1.024\ 0.909\ 0.61\ 0.32\ 0.16\ 3.23\ 0.00]$	g/l
$\mathbf{x}_{02}^{\text{T}} = [0.612\ 0.084\ 21.87\ 8.07\ 0.42\ 20.13\ 1.23]$	g/l
$\mathbf{x}_{03}^{\text{T}} = [15.446\ 0.002\ 0.74\ 0.19\ 0.05\ 1.63\ 0.18]$	g/l

Table 4
Parameter set resulting from identification: model parameters and their standard deviations

Parameter	(Unit)	Value	Standard deviation
Y_a	(g/g)	0.0736	0.0072
Y_m	(g/g)	0.214	0.0086
$\varphi_{h,max}$	(1/d)	3.30	0.70
$\varphi_{a,\max}$	(1/d)	1.41	0.29
$(ke_0)_m$	(1/d)	5.73	0.46
$k_{d,a}$	(1/d)	5.56×10^{-3}	1.59×10^{-3}
$k_{d,m}$	(1/d)	0.918	0.107
K_{X_S}	(g/l)	45.5	11.5
K_{S_S}	(g/l)	9.97	0.97
$K_{S_{\text{VFA}}}$	(g/l)	4.454	0.47
$p_{H,\text{opt}}$	(dimensionless)	7.95	0.15
Δp_K	(dimensionless)	1.99	0.14
Ω_{S_S}	(gCOD/g)	2.97	0.56
Ω_{X_S}	(gCOD/g)	1.34	0.09
$\Omega_{S_{\text{VFA}}}$	(gCOD/g)	1.00	0.15
Ω_{X_X}	(gCOD/g)	1.03	0.25
Γ_{S_S}	(mgTOC/g)	800	159
$\Gamma_{S_{\text{VFA}}}$	(mgTOC/g)	504	56
$\sigma_{y,\text{rel}}$	(dimensionless)	0.296	

Table 5
Measured waste concentrations (in g/l) in comparison with predicted values

Variable	Name	Measured	Predicted
COD_s	Chemical oxygen demand (dissolved)	4.17	4.90
COD_t	Chemical oxygen demand (total)	20.0	18.62
MiS	Material in suspension	21.31	19.92
TDE	Total dry extract	23.13	21.73
ODE	Organic dry extract	14.68	11.87
TOC	Total organic carbon (dissolved)	1.7	1.33
VFA	Volatile fatty acids	0.02	0.02

5.4. Numerical values

The solution of the parameter estimation is given in the Tables 3 and 4. The parameter values are obtained by minimisation of the cost function (26) with respect to the complete parameter vector including the experimental and the structural parameters.

Table 5 compares the measured with the predicted feed concentrations for the experiments 1–4.

5.5. Interpretation

The parameter values estimated by the optimization process lead to the following interpretations of the mathematical model:

- The yields of produced biomass referred to consumed substrate for both types of biomass are relatively low. Around ten to twenty mass percent of the substrates are converted into biomass.
- The high values for K_{X_S}, K_{S_S} and K_{S_S} indicate quasi-first-order kinetics of the hydrolysis, the acidogenisis and methanogenic step with respect to their limiting substrate, since the estimated respective substrate concentrations are always below these values. This is confirmed by unrealistically high maximum reaction rates (all above 2 l/d). The respective quasi-linear reaction constants are calculated then as the ratio of the maximum reaction rate $\varphi_{\max}$ and the saturation constant K and represent the slope of the Monod law at zero concentration.

$$k = \frac{\varphi_{\max}}{K}. \tag{30}$$

  The resulting constants are $k_h = 0.072$ l/gd, $k_a = 0.14$ l/gd and $k_{m,\max} = 1.29$ l/gd, respectively.
- The effective maximum growth rate of the p_H-dependent methanisation step is $\varphi_{m,\max}$ ($p_H = p_{H,\text{opt}} = 7.95$) = 5.61 1/d. For $p_H = 7$ the maximum growth rate decreases to 5.2 1/d and for $p_H = 6$ to 3.0 1/d.

Note that the parameter estimation in this case is delicate due to the important estimation load of the initial and feed conditions, which are not directly computable from the measurements, compared to the case of a directly measured state. The estimation of the initial states and the input conditions remains the critical task of the identification problem.

5.6. Model validation

A visual verification of the results is achieved by prediction of the model output using the parameter values computed in the identification step. As an example, the model prediction of the states and the measurements for experiment 4 is given in Figs. 2 and 3, respectively. The graphs show good agreement of the model with the experimental data, which are also shown for comparison together with their estimated 95% error bounds. In addition, the estimated feed concentration is displayed.

5.7. Discussion

According to Figs. 2 and 3, the model visually gives an appropriate representation of the anaerobic fermentation process.

From the evolution of the predicted concentration of the methanogenic biomass in Fig. 4, it is clearly visible that the p_H has some influence on the biomass growth in

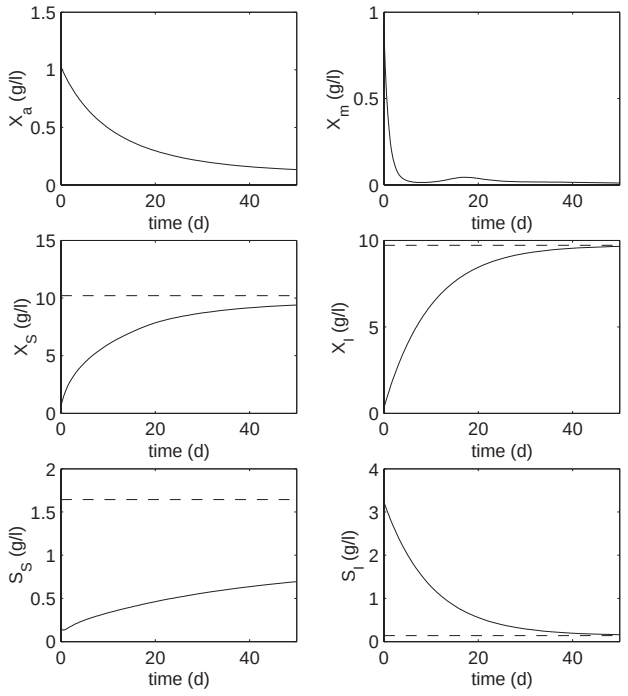

Fig. 2. Experiment 4 ($p_H = 7$, $S_{0,\text{in}} = 20$ gCOD/l): predicted states (solid) and feed concentrations (dashed).

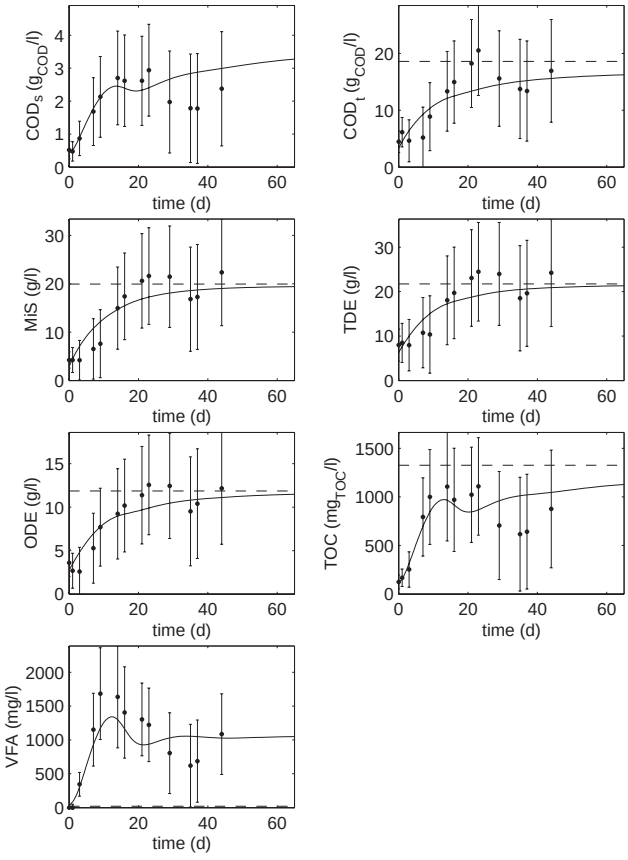

Fig. 3. Experiment 4 ($p_H = 7$, $S_{0,\text{in}} = 20$ gCODl): measurements (dots) with estimated 95% error bounds, predicted output (solid) and feed concentrations (dashed).

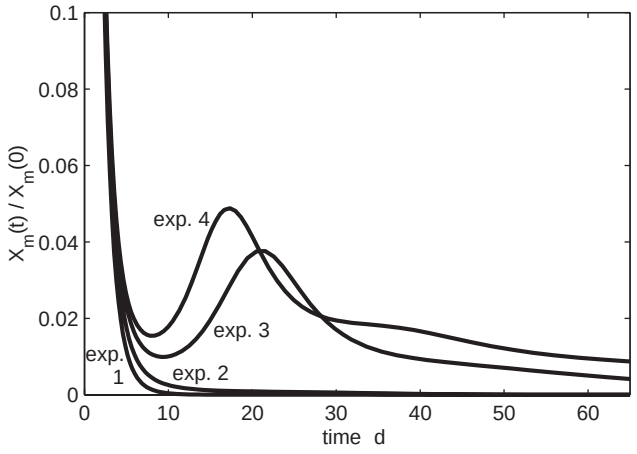

Fig. 4. Model prediction of methanogenic biomass concentration in experiments 1–4 ($S_{0,\mathrm{in}} = 20$ gCOD/l).

experiments 1–4. In the experiments 3 and 4, the biomass is not washed out of the reactor, as it is the case in experiments 1 and 2 due to the reduced reaction rate. Since the optimum $p_{H,\mathrm{opt}} = 7.95$ the consumption of the VFA and therefore the growth of biomass is greater in experiment 4 ($p_H = 7$) compared to experiment 1 ($p_H = 5.5$).

Fig. 3 shows another phenomenon occurring in most measurement plots: the fluctuation of the experimental data, which illustrates the magnitude of the measurement noise. This phenomenon is also quantified by the estimated relative standard measurement deviation, which is around 30%. Obviously, the measurement values are correlated, probably due to inaccuracies in the dilution of the samples for analysis or due to non-ideal mixing conditions of the reactor.

6. Statistical analysis

After the complete model identification, the confidence in the resulting set of parameters has to be analysed.

6.1. Measurement covariance

As the measurement errors are not known a priori, their estimation is implicitly included in the optimisation criterion. The estimated variances are calculated according to Eq. (27) and represent the elements in the diagonal covariance matrix $\boldsymbol{\Sigma}$.

6.2. Confidence and correlation

Fisher's information matrix

$$\mathbf{F}(\hat{\mathbf{p}}) = \underset{\mathbf{y}|\hat{\mathbf{p}}}{E}\left\{\left[\frac{\partial\{\ln P(\mathbf{y}|\mathbf{p})\}}{\partial\mathbf{p}}\right]\left[\frac{\partial\{\ln P(\mathbf{y}|\mathbf{p})\}}{\partial\mathbf{p}}\right]^{\mathrm{T}}\right\} \tag{31}$$

contains the sensitivities $(\partial/\partial\mathbf{p})\{\ln P\}$ of the log-likelihood function with respect to the estimated parameters at all sampling instants.

If the assumptions underlying the Gauss–Markov criterion are fulfilled, Fisher's information matrix is written in the simple form:

$$\mathbf{F}(\hat{\mathbf{p}}) = \sum_{i=1}^{n_t}\left[\left.\frac{\partial\mathbf{y}(t,\mathbf{p})}{\partial\mathbf{p}^{\mathrm{T}}}\right|_{t_i,\hat{\mathbf{p}}}\right]^{\mathrm{T}}\boldsymbol{\Sigma}_i^{-1}\left[\left.\frac{\partial\mathbf{y}(t,\mathbf{p})}{\partial\mathbf{p}^{\mathrm{T}}}\right|_{t_i,\hat{\mathbf{p}}}\right]. \tag{32}$$

The confidence in the solution in terms of the parameter covariance matrix can be estimated by the Cramér–Rao inequality

$$\mathbf{P} \geqslant \mathbf{F}(\hat{\mathbf{p}})^{-1}, \tag{33}$$

which becomes an equality only in the ideal case of an infinite number of data points (continuous measurement). It gives anyway an idea about the confidence intervals of the parameters.

The standard deviations σ_p of the parameters in Table 4 allow a satisfactory confidence in the determined set of parameters.

The correlation between parameters, i.e. the interplay between two parameters p_i and p_j in terms of their influence on the system behaviour, is quantified by the correlation matrix

$$\{\mathbf{P}^*\}_{ij} = \frac{\{\mathbf{P}\}_{ij}}{\sqrt{\{\mathbf{P}\}_{ii}\{\mathbf{P}\}_{jj}}} \tag{34}$$

fulfilling

$$-1 < \{\mathbf{P}^*\}_{ij} \leqslant 1. \tag{35}$$

Elements $\{\mathbf{P}^*\}_{ij}$ with an absolute value close to one indicate a strong correlation between the parameters p_i and p_j.

Applied to the identification results, the following parameters are correlated according to this criterion:

- the pair $\{\varphi_{h,\max}, K_{X_S}\}$ for the kinetics of the hydrolytic step is strongly correlated at a degree of 0.79;
- the tripel $\{(ke_0)_m, K_{S_{\mathrm{VFA}}}, k_{d,m}\}$ describing the methanogenic biomass shows correlations of degrees between 0.19 and 0.72;
- there is also a strong correlation between the two p_H parameters at a level of 0.74;
- the parameters Y_a, $\varphi_{a,\max}$, K_{S_S} and $k_{d,a}$ influencing the acidogenic biomass show only weak correlations with a maximum degree of 0.43.

7. Conclusions

The purpose of this paper is to discuss, through a real-case study, a procedure for model structure selection (and simplification) based on the examination of several macroscopic

reaction pathways (and in particular the number of biomass types that have to be distinguished) together with the available rare, noisy and global measurements. A simple model is developed for an aerobic waste treatment process, considering only two types of biomass, which is shown to be the maximum number of distinguishable micro-organisms from the available measurement data. At least the identifiability can be guaranteed in this case, even though the model is restricted to a very macroscopic view of the biodegradation process. Estimates for the parameters are calculated by minimising a maximum-likelihood criterion, which results in prediction curves in good agreement with the measurement data, even though the uncertainty on the estimated parameters remains at a relatively high level. However, compared to the quality of the measurements, the developed model together with the determined set of parameters seems to be an appropriate basis for further use in state observers, which is the intended application of the model.

Acknowledgements

The authors are very grateful to the Laboratoire de Biotechnologie de l'Environnement (LBE-INRA, Narbonne, France) for providing the experimental data.

References

Angelidaki, I., Ellegaard, L., & Ahring, B. (1999). A comprehensive model of bioconversion of complex substrates to biogas. *Biotechnology and Bioengineering*, *63*(3), 363–372.

Bailey, J. E., & Ollis, D. F. (1996). *Biochemical Engineering Fundamentals*. Chemical Engineering Series (2nd ed.). Singapore: McGraw-Hill.

Bernard, O., Hadj-Sadok, Z., & Dochain, D. (2000). Software sensors to monitor the dynamics of microbial communities: Application to anaerobic digestion. *Acta Biotheoretica*, *48*(3–4), 197–205.

Borja, R., Martín, A., Banks, C. J., Alonso, V., & Chica, A. (1995). A kinetic study of anaerobic digestion of olive mill wastewater at mesophilic and thermophilic temperatures. *Environmental Pollution*, *88*, 13–18.

Borzacconi, L., Lòpez, I., & Anido, C. (1997). Hydrolysis constant and VFA inhibition in acidogenic phase of msw anaerobic degradation. *Water Science and Technology*, *36*(6–7), 479–484.

Denac, M., Miguel, A., & Dunn, I. J. (1988). Modeling dynamic experiments on the anaerobic degradation of molasses wastewater. *Biotechnology and Bioengineering*, *31*, 1–10.

Fiestas Ros de Ursinos, J. A., & Borja-Padilla, R. (1996). Biomethanization. *International Biodeterioration & Biodegradation*, *38*, 145–153.

Gérin, F. (2000). Modèle mathematique pour la valorisation des déchets organiques solides. Mémoire. Conservatoire National des Arts et Métiers. Toulouse.

Goodwin, G. C., & Payne, R. L. (1977). *Dynamic system identification: Experiment design and data analysis. Mathematics in science and engineering* (Vol. 136). New York: Academic Press.

Hansen, K. H., Angelidaki, I., & Ahring, B. K. (1998). Anaerobic digestion of swine manure: Inhibition by ammonia. *Water Research*, *32*(1), 5–12.

Hill, D. T., & Barth, C. L. (1977). A dynamic model for simulation of animal waste digestion. *Journal of Water Pollution Control Federation*, *10*, 2129–2143.

Ingber, L. (1996). Adaptive simulated annealing (ASA): Lessons learned. *Control and Cybernetics*, *25*, 33–54.

Kiely, G., Tayfur, G., Dolan, C., & Tanji, K. K. (1997). Physical and mathematical modeling of anaerobic digestion of organic wastes. *Water Research*, *31*(3), 534–540.

Kirkpatrick, S., Gelatt Jr., C. D., & Vecchi, M. P. (1983). Optimization by simulated annealing. *Science*, *220*(4598), 671–680.

Lay, J. J., Li, Y. Y., Noike, T., Endo, J., & Ishimoto, S. (1997). Analysis of environmental factors affecting methane production from high-solids organic waste. *Water Science and Technology*, *36*(6–7), 493–500.

Monod, J. (1942). *Recherche sur la Croissance des Cultures Bacteriennes*. Paris: Herman Editions.

Nelder, J. A., & Mead, R. (1965). A simplex method for function minimization. *Comput. Journal*, *7*, 308–313.

Nocedal, J., & Wright, S. J. (1999). *Numerical optimization*. New York: Springer.

Powell, M. J. D. (1998). Direct search algorithms for optimization calculations. *Acta Numerica*. Volume 7, pp. 287–336.

Powell, M. J. D. (2000). *UOBYQA: Unconstrained optimisation by quadratic approximation*. Cambridge: University of Cambridge.

Simeonov, I., Momchev, F., & Grancharov, D. (1996). Dynamic modeling of mesophilic anaerobic digestion of animal waste. *Water Research*, *30*(5), 1087–1094.

Walter, É., Pronzato, L. (1997). Identification of parametric models from experimental data. *Communications and control engineering series*. Berlin–Heidelberg–New York: Springer.